

PUBLISHED VERSION

Gretel M. Png, Bernd M. Fischer, Dominique Appadoo, Ruth Plathe and Derek Abbott
Double-layered nitrocellulose membrane sample holding technique for THz and FIR spectroscopic measurements

Optics Express, 2015; 23(4):4997-5013

© 2015 Optical Society of America. Open Access - CC BY license.

Originally published at:

<http://doi.org/10.1364/OE.23.004997>

PERMISSIONS

<http://creativecommons.org/licenses/by/4.0/>



Attribution 4.0 International (CC BY 4.0)

This is a human-readable summary of (and not a substitute for) the [license](#).

[Disclaimer](#)



You are free to:

Share — copy and redistribute the material in any medium or format

Adapt — remix, transform, and build upon the material

for any purpose, even commercially.

The licensor cannot revoke these freedoms as long as you follow the license terms.

Under the following terms:



Attribution — You must give **appropriate credit**, provide a link to the license, and **indicate if changes were made**. You may do so in any reasonable manner, but not in any way that suggests the licensor endorses you or your use.

No additional restrictions — You may not apply legal terms or **technological measures** that legally restrict others from doing anything the license permits.

<http://hdl.handle.net/2440/100933>



A novel approach to nonperturbative renormalization of singlet and nonsinglet lattice operators



QCDSF Collaboration

A.J. Chambers^a, R. Horsley^b, Y. Nakamura^c, H. Perlt^{d,*}, P.E.L. Rakow^e, G. Schierholz^f,
A. Schiller^d, J.M. Zanotti^a

^a CSSM, Department of Physics, University of Adelaide, Adelaide, SA 5005, Australia

^b School of Physics and Astronomy, University of Edinburgh, Edinburgh EH9 3JZ, UK

^c RIKEN Advanced Institute for Computational Science, Kobe, Hyogo 650-0047, Japan

^d Institut für Theoretische Physik, Universität Leipzig, 04103 Leipzig, Germany

^e Theoretical Physics Division, Department of Mathematical Sciences, University of Liverpool, Liverpool L69 3BX, UK

^f Deutsches Elektronen-Synchrotron DESY, 22603 Hamburg, Germany

ARTICLE INFO

Article history:

Received 20 October 2014

Accepted 17 November 2014

Available online 20 November 2014

Editor: A. Ringwald

ABSTRACT

A novel method for nonperturbative renormalization of lattice operators is introduced, which lends itself to the calculation of renormalization factors for nonsinglet as well as singlet operators. The method is based on the Feynman–Hellmann relation, and involves computing two-point correlators in the presence of generalized background fields arising from introducing additional operators into the action. As a first application, and test of the method, we compute the renormalization factors of the axial vector current A_μ and the scalar density S for both nonsinglet and singlet operators for $N_f = 3$ flavors of SLiNC fermions. For nonsinglet operators, where a meaningful comparison is possible, perfect agreement with recent calculations using standard three-point function techniques is found.

© 2014 The Authors. Published by Elsevier B.V. This is an open access article under the CC BY license (<http://creativecommons.org/licenses/by/3.0/>). Funded by SCOAP³.

1. Introduction

To relate bare lattice results of hadron matrix elements and decay constants to phenomenological numbers, which are usually given in the $\overline{\text{MS}}$ scheme, the underlying operators need to be renormalized. This requires a nonperturbative method, because lattice perturbation theory is considered to be unreliable at present couplings.

A general nonperturbative method is the RI'-MOM subtraction scheme, which has been proposed in [1], with some refinements being added in [2]. Starting from the bare vertex function

$$\Gamma_{\mathcal{O}}(p) = S^{-1}(p)G_{\mathcal{O}}(p)S^{-1}(p), \quad (1)$$

where

$$G_{\mathcal{O}}(p) = \frac{1}{V} \sum_{x,y,z} e^{-ip(x-y)} \langle q(x)\mathcal{O}(z)\bar{q}(y) \rangle \quad (2)$$

is the quark Green function with operator insertion \mathcal{O} , and

$$S(p) = \frac{1}{V} \sum_{x,y} e^{-ip(x-y)} \langle q(x)\bar{q}(y) \rangle \quad (3)$$

is the quark propagator, the renormalized vertex function is defined by

$$\Gamma_{\mathcal{O}}^R(p) = Z_q^{-1} Z_{\mathcal{O}} \Gamma_{\mathcal{O}}(p). \quad (4)$$

Z_q denotes the quark field renormalization constant, which is taken as

$$Z_q(p) = \frac{\text{Tr}[-i \sum_{\lambda} \gamma_{\lambda} \sin(p_{\lambda}) S^{-1}(p)]}{12 \sum_{\rho} \sin^2(p_{\rho})}. \quad (5)$$

The renormalization factor $Z_{\mathcal{O}}(\mu)$ is determined by imposing the renormalization condition

$$\frac{1}{12} \text{Tr}[\Gamma_{\mathcal{O}}^R(p) \Gamma_{\mathcal{O}}^{\text{Born}}(p)^{-1}] = 1 \quad (6)$$

at the scale $p^2 = \mu^2$. Thus

$$Z_{\mathcal{O}}^{-1}(\mu) = \frac{1}{12} \text{Tr}[\Gamma_{\mathcal{O}}(\mu) \Gamma_{\mathcal{O}}^{\text{Born}}(\mu)^{-1}] Z_q^{-1}(\mu). \quad (7)$$

* Corresponding author.

E-mail address: perlt@itp.uni-leipzig.de (H. Perlt).

The lattice spacing a is assumed to be one, if not stated otherwise. V is the lattice volume.

The evaluation of $Z_{\mathcal{O}}$ requires the calculation of three-point functions. In the case of flavor singlet matrix elements this entails the computation of quark-line disconnected diagrams, which requires inversions of the fermion matrix at every lattice point and still leads to a poor signal to noise ratio. In this paper we propose an alternative method, based on the Feynman–Hellmann (FH) relation, which eliminates the issue of computing disconnected contributions directly at the expense of requiring the generation of additional ensembles of gauge field configurations. This essentially involves computing two-point correlators only in the presence of generalized background fields, which we show arise from introducing the operator \mathcal{O} into the action,

$$\mathcal{S} \rightarrow \mathcal{S}(\lambda) = \mathcal{S} - \lambda \sum_x \mathcal{O}(x), \quad \mathcal{S} = \mathcal{S}_F + \mathcal{S}_G, \quad (8)$$

where \mathcal{S}_F and \mathcal{S}_G are the fermionic and gauge field actions. A further advantage of this method is that the signal to noise ratio will be directly proportional to the external parameter λ , and thus can be controlled from the outside, as opposed to the standard three-point function calculation.

The quark propagators in (1) are calculated by inverting the fermion matrix, and so must be modified if we change the quark action. This change is straightforward to apply, only requiring a redefinition of the Dirac operator. In addition, any modification we make to the action in (8) should be included during the generation of the background gauge fields. By choosing to neglect either one of these modifications, we are able to individually isolate connected and disconnected contributions to the vertex function. Thus, modifications to the gauge configurations allow access to disconnected quantities, and modifications to the calculation of propagators allow access to connected quantities.

This paper follows previous work on hyperon sigma terms [3], the glue in the nucleon [4], and the spin structure of hadrons [5], already showing the potential of the Feynman–Hellmann approach to the calculation of hadron matrix elements. The outline of the paper is as follows. Section 2 describes the Feynman–Hellmann relation as relevant for the calculation of renormalization factors. In Sections 3.1 and 3.2 we apply the method to the computation of renormalization factors of the axial vector current A_μ and the scalar density S , respectively, for singlet and nonsinglet operators. The calculations are done with $N_f = 3$ flavors of SLiNC fermions [6,7]. Section 4 contains our conclusions.

2. The Feynman–Hellmann method

Throughout this paper we will consider quark-bilinear, flavor diagonal operators

$$\mathcal{O}(x) = \bar{q}(x)\Gamma q(x) \quad (9)$$

only, where Γ is some combination of gamma matrices. The generalization to operators including covariant derivatives is straightforward. The modified fermionic action then reads

$$\mathcal{S}_F(\lambda) = \sum_{q=u,d,s} \sum_x \bar{q}(x)[D + M - \lambda\Gamma]q(x), \quad (10)$$

where D is the lattice Dirac operator including the Wilson and clover terms, and M is the Wilson mass term. The latter is a diagonal 3×3 matrix in flavor space,

$$M = \begin{pmatrix} 1/2\kappa_u & & \\ & 1/2\kappa_d & \\ & & 1/2\kappa_s \end{pmatrix}. \quad (11)$$



Fig. 1. Diagrams contributing to the renormalization of quark-bilinear operators (inserted at point \times). The left figure shows the connected (nonsinglet) contribution, the right figure the disconnected (singlet minus nonsinglet) contribution. Gluon lines have been omitted.

One is mainly interested in renormalization factors in a mass-independent scheme, such as the $\overline{\text{MS}}$ scheme. To comply with that, we choose the quarks to be mass degenerate,

$$M = (1/2\kappa)\mathbb{1}, \quad \kappa_u = \kappa_d = \kappa_s \equiv \kappa, \quad (12)$$

and tune κ to its critical value, κ_c , at the end of the calculation. A better choice might be to only take the u and d quarks as mass-degenerate, $\kappa_u = \kappa_d \equiv \kappa_\ell$, and keep the sum of the quark masses fixed [7], $2/\kappa_\ell + 1/\kappa_s = \text{constant}$, while taking κ_ℓ to its critical value, $\kappa_{\ell,c}$. In that case we would have

$$M = \begin{pmatrix} 1/2\kappa_\ell & & \\ & 1/2\kappa_\ell & \\ & & 1/2\kappa_s \end{pmatrix}. \quad (13)$$

After integrating out the quark fields, the fermion propagator becomes

$$S(\lambda_{\text{sea}}, \lambda_{\text{val}}) = \frac{\int \mathcal{D}U [D + M - \lambda_{\text{val}}\Gamma]^{-1} \det[D + M - \lambda_{\text{sea}}\Gamma] \exp\{-\mathcal{S}_G(U)\}}{\int \mathcal{D}U \det[D + M - \lambda_{\text{sea}}\Gamma] \exp\{-\mathcal{S}_G(U)\}}, \quad (14)$$

where we differentiate between operator insertions in the quark propagator (λ_{val}) and the fermion determinant (λ_{sea}), to separate connected and disconnected diagrams eventually. In what follows Fourier transformation of $S(\lambda_{\text{sea}}, \lambda_{\text{val}})$ to momentum space is understood. For the sake of simplicity any dependence on external momenta will be omitted. Expanding the propagator in terms of $\lambda_{\text{sea}}, \lambda_{\text{val}}$ gives

$$\begin{aligned} S(\lambda_{\text{sea}}, \lambda_{\text{val}}) &= \langle [D + M]^{-1} \rangle + \lambda_{\text{val}} \langle [D + M]^{-1} \Gamma [D + M]^{-1} \rangle \\ &\quad - \lambda_{\text{sea}} \{ \langle [D + M]^{-1} \text{Tr}(\Gamma [D + M]^{-1}) \rangle \\ &\quad - \langle [D + M]^{-1} \rangle \langle \text{Tr}(\Gamma [D + M]^{-1}) \rangle \} \\ &\quad + O(\lambda_{\text{sea}}^2, \lambda_{\text{sea}}\lambda_{\text{val}}, \lambda_{\text{val}}^2), \end{aligned} \quad (15)$$

where the expectation values $\langle \dots \rangle$ refer to the unmodified action. By differentiating the quark propagator with respect to λ_{val} and λ_{sea} we obtain

$$\left. \frac{\partial S(0, \lambda_{\text{val}})}{\partial \lambda_{\text{val}}} \right|_{\lambda_{\text{val}}=0} = \langle [D + M]^{-1} \Gamma [D + M]^{-1} \rangle \equiv G_{\mathcal{O}}^{\text{con}} \quad (16)$$

and

$$\begin{aligned} \left. \frac{\partial S(\lambda_{\text{sea}}, 0)}{\partial \lambda_{\text{sea}}} \right|_{\lambda_{\text{sea}}=0} &= -\langle [D + M]^{-1} \text{Tr}(\Gamma [D + M]^{-1}) \rangle \\ &\quad + \langle [D + M]^{-1} \rangle \langle \text{Tr}(\Gamma [D + M]^{-1}) \rangle \equiv G_{\mathcal{O}}^{\text{dis}}, \end{aligned} \quad (17)$$

where $G_{\mathcal{O}}^{\text{con}}$ and $G_{\mathcal{O}}^{\text{dis}}$ are the fermion-line connected and disconnected quark Green functions, respectively. In Fig. 1 we sketch both types of contributions. Note that (17) only includes diagrams where gluon lines connect the quark loop to the external legs. The

unitary (full) quark Green function, including both connected and disconnected diagrams, is given by

$$G_{\mathcal{O}} = \left. \frac{\partial S(\lambda, \lambda)}{\partial \lambda} \right|_{\lambda=0} = G_{\mathcal{O}}^{\text{con}} + G_{\mathcal{O}}^{\text{dis}}. \quad (18)$$

By multiplying $G_{\mathcal{O}}$ and $G_{\mathcal{O}}^{\text{con}}$ with the inverse unmodified propagator from left and right we obtain singlet,

$$\Gamma_{\mathcal{O}}^{\text{S}} = S(0, 0)^{-1} G_{\mathcal{O}} S(0, 0)^{-1}, \quad (19)$$

and nonsinglet,

$$\Gamma_{\mathcal{O}}^{\text{NS}} = S(0, 0)^{-1} G_{\mathcal{O}}^{\text{con}} S(0, 0)^{-1}, \quad (20)$$

vertex functions. The corresponding renormalization factors are then given by

$$Z_{\mathcal{O}}^{\text{S}-1} = \frac{1}{12} \text{Tr}[\Gamma_{\mathcal{O}}^{\text{S}} \Gamma_{\mathcal{O}}^{\text{Born}-1}] Z_q^{-1} \quad (21)$$

and

$$Z_{\mathcal{O}}^{\text{NS}-1} = \frac{1}{12} \text{Tr}[\Gamma_{\mathcal{O}}^{\text{NS}} \Gamma_{\mathcal{O}}^{\text{Born}-1}] Z_q^{-1}. \quad (22)$$

We could have started from singlet and nonsinglet operators with a single parameter λ , as stated in (8), instead of differentiating between operator insertions in propagator and determinant. For example

$$\mathcal{O}^{\text{S}}(x) = \sum_{q=u,d,s} \bar{q}(x) \Gamma q(x), \quad (23)$$

$$\mathcal{O}^{\text{NS}}(x) = \bar{u}(x) \Gamma u(x) - \bar{d}(x) \Gamma d(x). \quad (24)$$

For the singlet operator (23) nothing changes. The nonsinglet operator (24) would contribute $O(\lambda^2)$ to the determinant for either choice of M , Eqs. (12) and (13), which leaves us with

$$\left. \frac{\partial S(\lambda, \lambda)}{\partial \lambda} \right|_{\lambda=0} = G_{\mathcal{O}}^{\text{con}}. \quad (25)$$

We have just added the singlet operator to the action. If we also added a term $\lambda_{\text{sea}}^{\text{NS}} \mathcal{O}^{\text{NS}}$ it would not change anything, the nonsinglet operator would contribute to the determinant at $O((\lambda_{\text{sea}}^{\text{NS}})^2)$, and so not change the derivative at $\lambda = 0$.

3. Numerical results and tests

We shall now apply the Feynman–Hellmann method of nonperturbative renormalization to the axial vector current and the scalar density. It is convenient to introduce the primitive

$$\Lambda_{\mathcal{O}}(\lambda_{\text{sea}}, \lambda_{\text{val}}) = \frac{1}{12} \text{Tr}[S(0, 0)^{-1} S(\lambda_{\text{sea}}, \lambda_{\text{val}}) S(0, 0)^{-1} \Gamma_{\mathcal{O}}^{\text{Born}-1}]. \quad (26)$$

Expanding the propagator $S(\lambda_{\text{sea}}, \lambda_{\text{val}})$ in terms of $\lambda_{\text{sea}}, \lambda_{\text{val}}$, using (15), we obtain

$$\Lambda_{\mathcal{O}}(\lambda_{\text{sea}}, \lambda_{\text{val}}) = a_0 + a_{\text{sea}} \lambda_{\text{sea}} + a_{\text{val}} \lambda_{\text{val}} + O(\lambda_{\text{sea}}^2, \lambda_{\text{sea}} \lambda_{\text{val}}, \lambda_{\text{val}}^2). \quad (27)$$

The coefficients a_{sea} and a_{val} are what we need to compute,

$$Z_{\mathcal{O}}^{\text{NS}} = \frac{Z_q}{a_{\text{val}}}, \quad Z_{\mathcal{O}}^{\text{S}} = \frac{Z_q}{a_{\text{val}} + a_{\text{sea}}}. \quad (28)$$

The proposed method involves the computation of two-point functions only. In the case of nonsinglet operators no extra gauge field configurations need to be generated. The parameters $\lambda_{\text{sea}}, \lambda_{\text{val}}$

Table 1

The parameters λ_{val} and λ_{sea} employed in the simulations.

λ_{val}	λ_{sea}			
-0.0125	-0.03	0.0	0.00625	0.0125
-0.00625	-0.03	0.0	0.00625	0.0125
-0.003125	-0.03	0.0	0.00625	0.0125
0.0	-0.03	0.0	0.00625	0.0125
0.03	-0.03	0.0	0.00625	0.0125

should be chosen large enough to give a strong signal, but small enough so that $\Lambda_{\mathcal{O}}$ can be fitted by a low-order polynomial in $\lambda_{\text{sea}}, \lambda_{\text{val}}$.

The calculations are performed on $32^3 \times 64$ lattices at $\beta = 5.50$, corresponding to a lattice spacing of $a = 0.074(2)$ fm [8]. We will use momentum sources [2] throughout the calculation. Using twisted boundary conditions, the momenta are chosen to be strictly diagonal, $p = (\rho, \rho, \rho, \rho)$. They are $(ap)^2 = 0.1542, 0.6169, 1.3879, 2.4674, 3.8553, 5.5517, 7.5564$ and 9.8696 , as given in the first column of Table III in [9]. This choice of momenta will leave us with $O((ap)^2)$ scaling violations only, but with no direction-specific corrections, which we consider a great advantage.

We are finally interested in renormalization factors in the RGI and $\overline{\text{MS}}$ schemes. The conversion from the RI'-MOM scheme to the RGI scheme is preferably done by a two-step process [10]

$$Z_{\mathcal{O}}^{\text{RGI}} = \Delta Z_{\mathcal{O}}^{\text{MOM}}(\mu) Z_{\text{RI}'\text{-MOM}}^{\text{MOM}}(\mu) Z_{\mathcal{O}}^{\text{RI}'\text{-MOM}}(\mu), \quad (29)$$

which we follow here. The renormalization factors in the $\overline{\text{MS}}$ scheme are given by

$$Z_{\mathcal{O}}^{\overline{\text{MS}}}(\mu) = \Delta Z_{\mathcal{O}}^{\overline{\text{MS}}}(\mu)^{-1} Z_{\mathcal{O}}^{\text{RGI}}. \quad (30)$$

The conversion factors $\Delta Z_{\mathcal{O}}^{\text{MOM}}(\mu)$, $Z_{\text{RI}'\text{-MOM}}^{\text{MOM}}(\mu)$ and $\Delta Z_{\mathcal{O}}^{\overline{\text{MS}}}(\mu)$ are computed in continuum perturbation theory [12,13]. They depend on $\Lambda_{\overline{\text{MS}}}$, which we choose as $\Lambda_{\overline{\text{MS}}} = 339$ MeV [11].

3.1. Axial vector current

In order to proceed with the determination of the renormalization constant of the axial current, we add the third component of the axial current

$$A_3(x) = \bar{q}(x) \gamma_3 \gamma_5 q(x), \quad (31)$$

to the action (8). This operator is γ_5 -hermitean, and hence suitable for inclusion as part of the Hybrid Monte Carlo when generating the new sets of gauge configurations required for the determination of the disconnected contributions. The simulations are performed at the SU(3) flavor symmetric point $\kappa_u = \kappa_d = \kappa_s = 0.12090$ [7], corresponding to $m_{\pi} = m_K = 465$ MeV, for five different λ_{val} values with four different values of λ_{sea} each. The actual run parameters are listed in Table 1.

In Fig. 2 we show our results for $\Lambda_A(\lambda_{\text{sea}}, \lambda_{\text{val}})$ and the difference $\Lambda_A(\lambda_{\text{sea}}, \lambda_{\text{val}}) - \Lambda_A(0, \lambda_{\text{val}})$ for one of our intermediate momenta, $(ap)^2 = 2.4674$. Within the range of parameters we have explored, $\Lambda_A(\lambda_{\text{sea}}, \lambda_{\text{val}})$ (shown in the top figure) appears to be a linear function of both λ_{sea} and λ_{val} . The figure indicates that $a_{\text{sea}} \ll a_{\text{val}}$ for the axial vector current. In spite of being a rather small number, the disconnected contribution a_{sea} can be computed very accurately by our method. This is illustrated by the difference $\Lambda_A(\lambda_{\text{sea}}, \lambda_{\text{val}}) - \Lambda_A(0, \lambda_{\text{val}}) = a_{\text{sea}} \lambda_{\text{sea}} + O(\lambda_{\text{sea}}^2, \lambda_{\text{sea}} \lambda_{\text{val}}, \lambda_{\text{val}}^2)$ (shown in the bottom figure). It helps the fit that higher order corrections are small. Similar results are found for the other momenta. We thus may fit our data for $\Lambda_A(\lambda_{\text{sea}}, \lambda_{\text{val}})$ by the ansatz

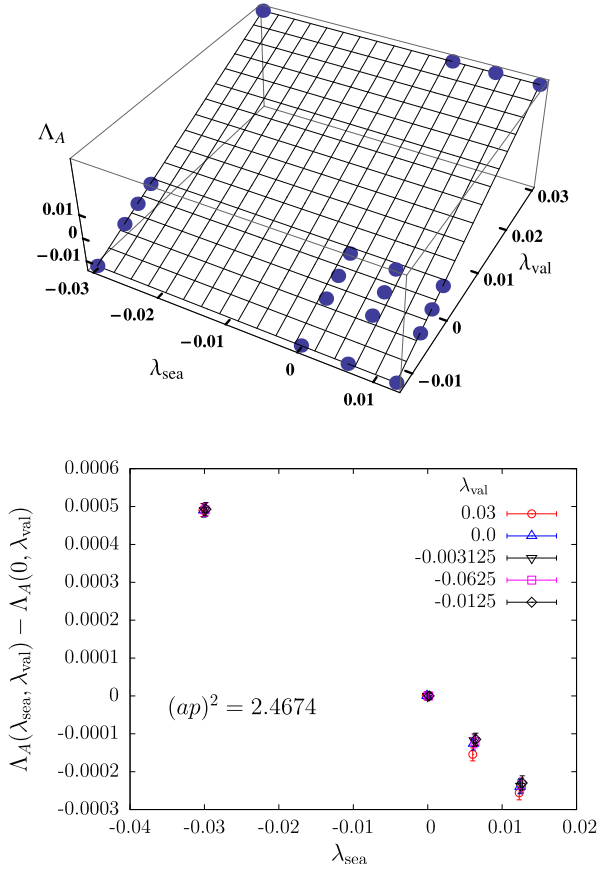


Fig. 2. Top panel: $\Lambda_A(\lambda_{\text{sea}}, \lambda_{\text{val}})$ as a function of λ_{sea} and λ_{val} for $(ap)^2 = 2.4674$. Bottom panel: The difference $\Lambda_A(\lambda_{\text{sea}}, \lambda_{\text{val}}) - \Lambda_A(0, \lambda_{\text{val}}) = a_{\text{sea}}\lambda_{\text{sea}} + O(\lambda_{\text{sea}}^2, \lambda_{\text{sea}}\lambda_{\text{val}}, \lambda_{\text{val}}^2)$ as a function of λ_{sea} , for $(ap)^2 = 2.4674$.

$$\Lambda_A(\lambda_{\text{val}}, \lambda_{\text{sea}}) = a_0 + a_{\text{sea}}\lambda_{\text{sea}} + a_{\text{val}}\lambda_{\text{val}}. \quad (32)$$

This is done for each momentum source separately. The result is shown in Fig. 3. From a_{sea} and a_{val} , together with Z_q defined in (5), we obtain the renormalization factors in the RI'-MOM scheme. The result is given in Fig. 4 (left panel) for singlet and nonsinglet operators. The obvious question now is: how does that result compare with previous results using standard methods? In [9] we have computed the nonsinglet renormalization factor from three-point functions using the same action. We compare that result with the Feynman–Hellmann result of this paper in Fig. 4 (right panel). We find perfect agreement.

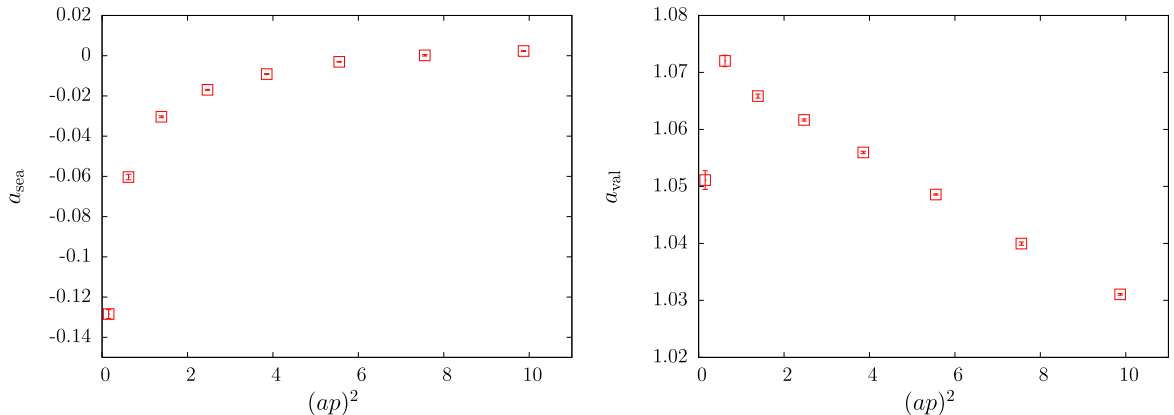


Fig. 3. The coefficients a_{sea} and a_{val} as a function of $(ap)^2$.

Let us now convert our numbers to the RGI and $\overline{\text{MS}}$ schemes, using (29) and (30). In the nonsinglet case $\Delta Z_A^{\text{MOM}}(\mu) = \Delta Z_A^{\overline{\text{MS}}}(\mu) = 1$, as the anomalous dimension is zero. In the singlet case both $\Delta Z_A^{\text{MOM}}(\mu)$ and $\Delta Z_A^{\overline{\text{MS}}}(\mu)$ are nonzero and depend on the scale $\mu = \sqrt{p^2}$ [12,13]. In Fig. 5 we show Z_A^{RGI} for both singlet and nonsinglet operators. We restrict ourselves to $(ap)^2 \geq 2$. Below that long-distance effects become dominant. As in [9], the nonsinglet data show scaling violations which can be approximated by a linear ansatz in $(ap)^2$. We fit the singlet data by a quadratic ansatz. The result is

$$Z_A^{\text{RGI,NS}} = 0.8458(8), \quad Z_A^{\text{RGI,S}} = 0.9285(36). \quad (33)$$

The renormalization factors $Z_A^{\overline{\text{MS}}}(\mu)$ are obtained by multiplying the numbers in (33) by $\Delta Z_A^{\overline{\text{MS}}}(\mu)^{-1}$. They are scale dependent. At $\mu = 2$ GeV we obtain

$$Z_A^{\overline{\text{MS,NS}}} = 0.8458(8), \quad Z_A^{\overline{\text{MS,S}}} = 0.8662(34). \quad (34)$$

The difference of singlet and nonsinglet renormalization factors of the axial vector current turns out to be small. That is not surprising since it is already known that in perturbation theory singlet and nonsinglet numbers start to depart only at two loops [14]. The good news is that the Feynman–Hellmann method enables us to compute the disconnected contribution a_{sea} , in spite of being a factor of 20 smaller than the connected one a_{val} , to an unprecedented precision of less than a percent.

It should be remembered that our results (33) and (34) refer to the flavor symmetric point $\kappa_\ell = \kappa_s = 0.12090$. To extrapolate the renormalization factors to the chiral limit, we would have to perform more simulations with the modified fermionic action at smaller quark masses.

3.2. Scalar density

We now turn to the scalar density

$$S(x) = \bar{q}(x)q(x). \quad (35)$$

In this case the modification of the fermionic action, $S_F \rightarrow S_F - \lambda \sum_x S(x)$, is equivalent to changing the κ values to $\kappa + \delta$, with $\delta = 2\lambda\kappa^2/(1 - 2\lambda\kappa)$. As before, $\kappa_u = \kappa_d = \kappa_s$ is assumed. We allow the kappa values of sea and valence quarks to be different, and express the primitive (26) in terms of the new variables δ_{sea} and δ_{val} . Expanding $\Lambda_5(\delta_{\text{sea}}, \delta_{\text{val}})$ about the reference point $(\kappa_{\text{sea}}, \kappa_{\text{val}})$ then gives

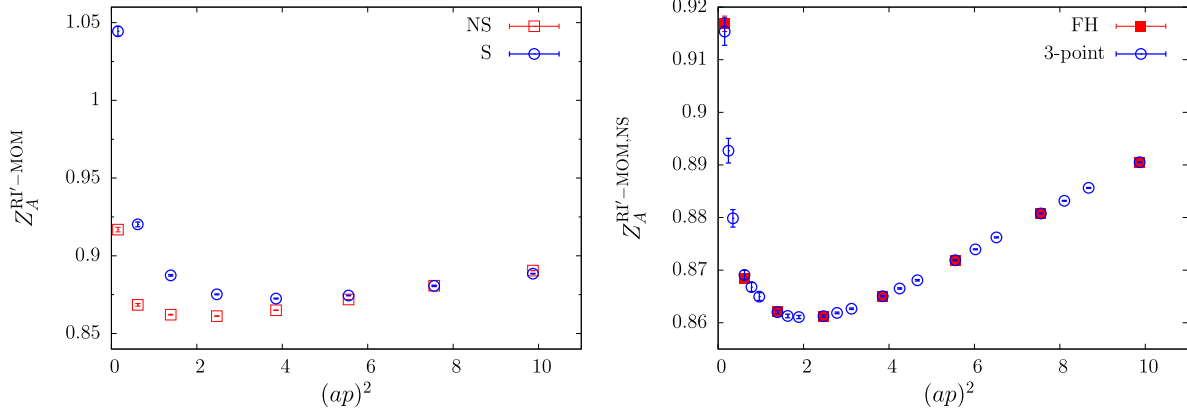


Fig. 4. Left panel: singlet and nonsinglet renormalization factors Z_A in the RI'-MOM scheme at $\kappa_{\text{sea}} = 0.12090$. Right panel: comparison of the nonsinglet renormalization factor Z_A in the RI'-MOM scheme obtained from the Feynman-Hellmann (FH) approach (this work) and the three-point function method [9].

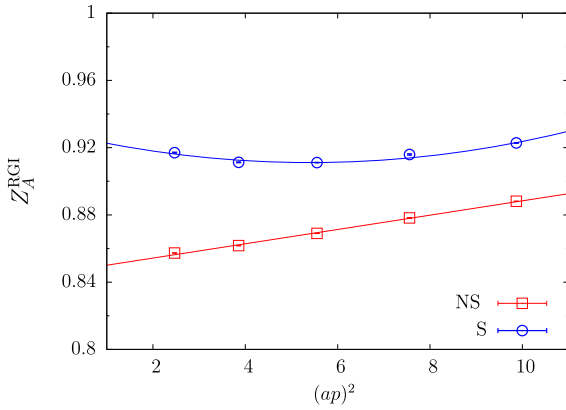


Fig. 5. Singlet and nonsinglet renormalization factors in the RGI scheme, together with a linear (quadratic) fit to $2 \leq (ap)^2 \leq 10$ for the nonsinglet (singlet) Z_A^{RGI} .

Table 2

The parameters of background field configurations, κ_{val} and κ_{sea} , used in the calculation of the scalar density.

κ_{val}				κ_{sea}
0.120900	0.120920	0.120950	0.120990	0.120900
	0.190920			0.120920
		0.120950		0.120950
			0.120990	0.120990
			0.121021	0.121021

$$\Lambda_S(\delta_{\text{sea}}, \delta_{\text{val}}) = a_0 + (a_{\text{sea}}/2\kappa_{\text{sea}}^2)\delta_{\text{sea}} + (a_{\text{val}}/2\kappa_{\text{val}}^2)\delta_{\text{val}} + O(\delta_{\text{sea}}^2, \delta_{\text{sea}}\delta_{\text{val}}, \delta_{\text{val}}^2). \quad (36)$$

Here we can draw on existing background gauge field configurations [7]. In Table 2 we list the κ parameters of the configurations used in this calculation.

In Fig. 6 we show $\Lambda_S(\delta, \delta)$ as a function of δ at the reference point $\kappa_{\text{ref}} = \kappa_{\text{sea}} = \kappa_{\text{val}} = 0.12090$ for one of our intermediate fit momenta, $(ap)^2 = 7.5564$. To a good approximation, the data lie on a straight line. From the slope at $\delta = 0$ ($\kappa = \kappa_{\text{ref}}$) we obtain the singlet renormalization factor in the RI'-MOM scheme,

$$\left. \frac{\partial \Lambda_S(\delta, \delta)}{\partial \delta} \right|_{\delta=0} = \frac{a_{\text{sea}} + a_{\text{val}}}{2\kappa_{\text{ref}}^2} = \frac{Z_q}{2\kappa_{\text{ref}}^2 Z_S^{\text{RI'-MOM,S}}}. \quad (37)$$

Repeating the calculation at $\kappa_{\text{ref}} = 0.12092, 0.12095, 0.12099$ and 0.121021 , with pion masses ranging from 465 MeV ($\kappa = 0.12090$) to 290 MeV ($\kappa = 0.121021$) [9], we can perform the chiral extrapolation of $Z_S^{\text{RI'-MOM,S}}$. In Fig. 7 we show $Z_S^{\text{RI'-MOM,S}}$ as a function of

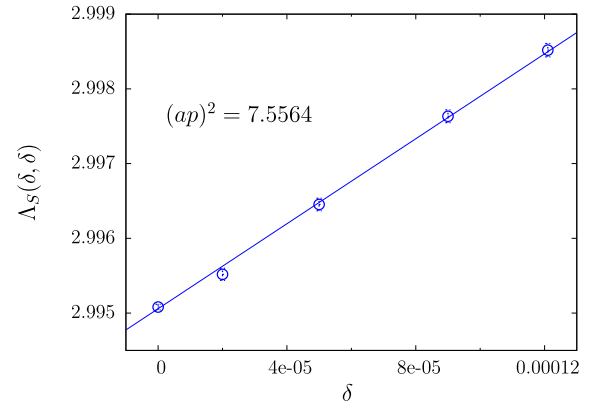


Fig. 6. The primitive $\Lambda_S(\delta, \delta)$ at the reference point $\kappa_{\text{ref}} = \kappa_{\text{sea}} = \kappa_{\text{val}} = 0.12090$ as a function of δ for $(ap)^2 = 7.5564$, together with a linear fit.

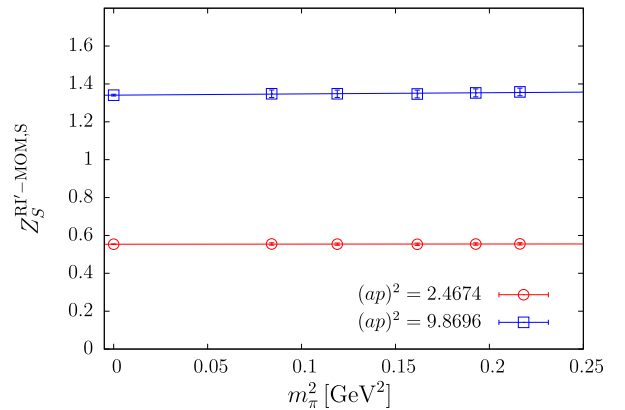


Fig. 7. The singlet renormalization factor in the RI'-MOM scheme as a function of m_π^2 for two momenta, $(ap)^2 = 2.4674$ and 9.869 , together with a linear extrapolation to the chiral limit.

m_π^2 for two different momenta, together with the extrapolated values. Singlet $Z_S^{\text{RI'-MOM,S}}$ is practically independent of the pion mass.

To convert $Z_S^{\text{RI'-MOM,S}}$ to the RGI and $\overline{\text{MS}}$ schemes we proceed as before. In Fig. 8 we show $Z_S^{\text{RGI,S}}$. The data show scaling violations approximately linear in $(ap)^2$, which appear to be common to all our results [9]. We restrict ourselves to $(ap)^2 \geq 2$ and fit the data by the ansatz $Z_S^{\text{RGI,S}} + C(ap)^2$. The result is

$$Z_S^{\text{RGI,S}} = 0.2617(35), \quad (38)$$

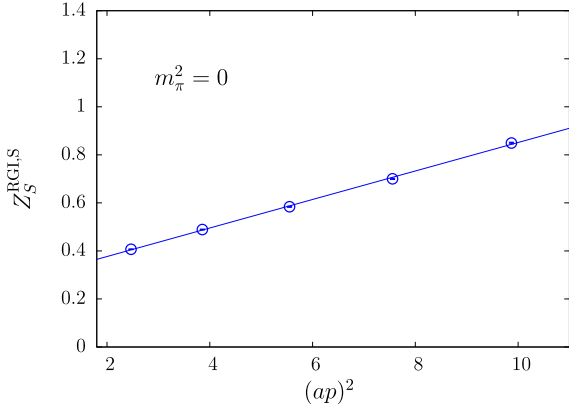


Fig. 8. The singlet renormalization factor $Z_S^{\text{RGI,S}}$ in the chiral limit, together with a linear fit to $2 \leq (ap)^2 \leq 10$.

which upon conversion to the $\overline{\text{MS}}$ scheme at $\mu = 2$ GeV gives

$$Z_S^{\overline{\text{MS}},S} = 0.3544(48). \quad (39)$$

In contrast to (33) and (34), both numbers refer to the chiral limit.

As a further test, we have computed the nonsinglet renormalization factor $Z_S^{\text{RI}^{\prime\text{-MOM}},\text{NS}}$ at $\kappa_{\text{ref}} = 0.12090$ and compared the outcome with our previous result from three-point functions [9]. We find perfect agreement, as before.

Using raw momentum data from [9] we found in the chiral limit

$$Z_S^{\text{RGI,NS}} = 0.5635(61) \quad (40)$$

and

$$Z_S^{\overline{\text{MS}},\text{NS}} = 0.7631(82) \quad \text{at } \mu = 2 \text{ GeV}, \quad (41)$$

giving

$$r_S = \frac{Z_S^{\text{RGI,NS}}}{Z_S^{\text{RGI,S}}} = \frac{Z_S^{\overline{\text{MS}},\text{NS}}}{Z_S^{\overline{\text{MS}},S}} = 2.15(4). \quad (42)$$

Note that $\Delta Z_S^{\text{RGI}}(\mu) = \Delta Z_S^{\overline{\text{MS}}}(\mu)$. In continuum perturbation theory and for chiral fermions $r_S = 1$. The deviation from one is an artifact of Wilson-type fermions. In [15] it was found that r_S rapidly approaches $r_S = 1$ as the lattice spacing is decreased. An independent estimate of r_S can be obtained from the ratio of valence to sea quark masses [7]. An updated value is $r_S = 1.82(8)$, which is in reasonable agreement with the result (42).

4. Conclusions

We have demonstrated that the Feynman–Hellmann method is an effective approach to calculating renormalization factors. For nonsinglet operators no additional gauge field configurations have to be generated. For singlet operators it appears that only a couple of different background field strengths need to be realized in order to make an accurate and precise calculation. We have demonstrated this through the determination of singlet and nonsinglet renormalization factors of the axial vector current and the scalar

density. Simulations of the axial vector current at smaller quark masses are in progress.

There is room for improvement. The renormalization factors show scaling violations in $(ap)^2$, which has puzzled us already in [9]. So far we have worked with unimproved quark propagators. Improving off-shell quark propagators should be simpler than improving three-point functions. Our goal is to remove lattice artifacts as far as possible. A first step in this direction has been taken in [16].

Acknowledgements

This work has been partly supported by the Deutsche Forschungsgemeinschaft, Grant SCHI 422/9-1, and the Australian Research Council, Grants FT100100005 and DP140103067. The numerical calculations were carried out on the BlueGeneQ at NIC (Jülich, Germany), on the BlueGeneQ at EPCC (Edinburgh, UK) using DIRAC2 resources, and on the Cray XC30 at HLRN (Berlin and Hannover, Germany). Some of the simulations were undertaken on the NCI National Facility (Canberra, Australia), which is supported by the Australian Commonwealth Government.

References

- [1] G. Martinelli, C. Pittori, C.T. Sachrajda, M. Testa, A. Vladikas, Nucl. Phys. B 445 (1995) 81, arXiv:hep-lat/9411010.
- [2] M. Göckeler, R. Horsley, H. Oelrich, H. Perlt, D. Petters, P.E.L. Rakow, A. Schäfer, G. Schierholz, A. Schiller, Nucl. Phys. B 544 (1999) 699, arXiv:hep-lat/9807044.
- [3] R. Horsley, Y. Nakamura, H. Perlt, D. Pleiter, P.E.L. Rakow, G. Schierholz, A. Schiller, H. Stüben, F. Winter, J.M. Zanotti, Phys. Rev. D 85 (2012) 034506, arXiv:1110.4971 [hep-lat].
- [4] R. Horsley, R. Millo, Y. Nakamura, H. Perlt, D. Pleiter, P.E.L. Rakow, G. Schierholz, A. Schiller, F. Winter, J.M. Zanotti, Phys. Lett. B 714 (2012) 312, arXiv:1205.6410 [hep-lat].
- [5] A.J. Chambers, R. Horsley, Y. Nakamura, H. Perlt, D. Pleiter, P.E.L. Rakow, G. Schierholz, A. Schiller, H. Stüben, R.D. Young, J.M. Zanotti, Phys. Rev. D 90 (2014) 014510, arXiv:1405.3019 [hep-lat].
- [6] N. Cundy, M. Göckeler, R. Horsley, T. Kaltenbrunner, A.D. Kennedy, Y. Nakamura, H. Perlt, D. Pleiter, P.E.L. Rakow, A. Schäfer, G. Schierholz, A. Schiller, H. Stüben, J.M. Zanotti, Phys. Rev. D 79 (2009) 094507, arXiv:0901.3302 [hep-lat].
- [7] W. Bietenholz, V. Bornyakov, M. Göckeler, R. Horsley, W.G. Lockhart, Y. Nakamura, H. Perlt, D. Pleiter, P.E.L. Rakow, G. Schierholz, A. Schiller, T. Streuer, H. Stüben, F. Winter, J.M. Zanotti, Phys. Rev. D 84 (2011) 054509, arXiv:1102.5300 [hep-lat].
- [8] R. Horsley, J. Najjar, Y. Nakamura, H. Perlt, D. Pleiter, P.E.L. Rakow, G. Schierholz, A. Schiller, H. Stüben, J.M. Zanotti, PoS LATTICE 2013 (2013) 249, arXiv:1311.5010 [hep-lat].
- [9] M. Constantinou, R. Horsley, H. Panagopoulos, H. Perlt, P.E.L. Rakow, G. Schierholz, A. Schiller, J.M. Zanotti, arXiv:1408.6047 [hep-lat].
- [10] M. Göckeler, R. Horsley, Y. Nakamura, H. Perlt, D. Pleiter, P.E.L. Rakow, A. Schäfer, G. Schierholz, A. Schiller, H. Stüben, J.M. Zanotti, Phys. Rev. D 82 (2010) 114511, arXiv:1003.5756 [hep-lat]; M. Göckeler, R. Horsley, Y. Nakamura, H. Perlt, D. Pleiter, P.E.L. Rakow, A. Schäfer, G. Schierholz, A. Schiller, H. Stüben, J.M. Zanotti, Phys. Rev. D 86 (2012) 099903 (Erratum).
- [11] S. Aoki, Y. Aoki, C. Bernard, T. Blum, G. Colangelo, M. Della Morte, S. Dürr, A.X. El Khadra, et al., arXiv:1310.8555 [hep-lat].
- [12] K.G. Chetyrkin, J.H. Kühn, Z. Phys. C 60 (1993) 497.
- [13] S.A. Larin, Phys. Lett. B 303 (1993) 113, arXiv:hep-ph/9302240.
- [14] A. Skouroupathis, H. Panagopoulos, Phys. Rev. D 79 (2009) 094508, arXiv:0811.4264 [hep-lat].
- [15] M. Göckeler, R. Horsley, A.C. Irving, D. Pleiter, P.E.L. Rakow, G. Schierholz, H. Stüben, Phys. Lett. B 639 (2006) 307, arXiv:hep-ph/0409312.
- [16] S. Capitani, M. Göckeler, R. Horsley, H. Perlt, P.E.L. Rakow, G. Schierholz, A. Schiller, Nucl. Phys. B 593 (2001) 183, arXiv:hep-lat/0007004.